

Article

Use of Lignite as a Low-Cost Material for Cadmium and Copper Removal from Aqueous Solutions: Assessment of Adsorption Characteristics and Exploration of Involved Mechanisms

Salah Jellali ^{1,*}, Ahmed Amine Azzaz ² , Mejdi Jeguirim ² , Helmi Hamdi ³ and Ammar Mlayah ⁴

¹ PEIE Research Chair for the Development of Industrial Estates and Free Zones, Center for Environmental Studies and Research (CESAR), Sultan Qaboos University, Al-Khoud, 123 Muscat, Oman

² The institute of Materials Science of Mulhouse (IS2M), University of Haute Alsace, University of Strasbourg, CNRS, UMR 7361, F-68100 Mulhouse, France; amine.azzaz@uha.fr (A.A.A.); mejdi.jeguirim@uha.fr (M.J.)

³ Center for Sustainable Development, College of Arts and Sciences, Qatar University, P.O. Box 2713, Doha, Qatar; hhamdi@qu.edu.qa

⁴ Georesources laboratory, Water Research and Technologies Center (CERTe), Echo park of Borj Cedria, Carthage University, P.O. Box 273, Soliman 8020, Tunisia; ammarmlayah17@gmail.com

* Correspondence: s.jellali@squ.edu.om

Abstract: Lignite, as an available and low-cost material, was tested for cadmium (Cd) and copper (Cu) removal from aqueous solutions under various static experimental conditions. Experimental results showed that the removal efficiency of both metals was improved by increasing their initial concentrations, adsorbent dosage and aqueous pH values. The adsorption kinetic was very rapid for Cd since about 78% of the totally adsorbed amounts were removed after a contact time of only 1 min. For Cd and Cu, the kinetic and isothermal data were well fitted with pseudo-second order and Freundlich models, respectively, which suggests that Cd/Cu removal by lignite occurs heterogeneously on multilayers surfaces. The maximum Langmuir's adsorption capacities of Cd and Cu were assessed to 38.0 and 21.4 mg g⁻¹ and are relatively important compared to some other lignites and raw natural materials. Results of proximate, scanning electron microscopy/energy dispersive X-ray spectroscopy (SEM/EDS), Fourier transform infrared spectroscopy (FTIR) and X-Ray diffraction (XRD) showed that the removal of these metals occurs most likely through a combination of cation exchange and complexation with specific functional groups. The relatively high adsorption capacity of the used lignite promotes its future use as a low cost material for Cd and Cu removal from effluents, and possibly for other heavy metals or groups of pollutants.

Keywords: lignite; heavy metals; adsorption; batch; isotherm; mechanism



Citation: Jellali, S.; Azzaz, A.A.; Jeguirim, M.; Hamdi, H.; Mlayah, A. Use of Lignite as a Low-Cost Material for Cadmium and Copper Removal from Aqueous Solutions: Assessment of Adsorption Characteristics and Exploration of Involved Mechanisms. *Water* **2021**, *13*, 164. <https://doi.org/10.3390/w13020164>

Received: 13 December 2020

Accepted: 6 January 2021

Published: 12 January 2021

Publisher's Note: MDPI stays neutral with regard to jurisdictional claims in published maps and institutional affiliations.



Copyright: © 2021 by the authors. Licensee MDPI, Basel, Switzerland. This article is an open access article distributed under the terms and conditions of the Creative Commons Attribution (CC BY) license (<https://creativecommons.org/licenses/by/4.0/>).

1. Introduction

The contamination of water resources by heavy metals contained in industrial effluents is an important worldwide concern due to their toxicity, low biodegradability and high accumulation capacity in water-living organisms [1]. When transferred to humans through the food chain, these metals could be accumulated in various body organs and tissues causing life-threatening illness and possible damages to vital systems [1]. Cadmium and copper are among the most toxic heavy metals. Indeed, exposure to cadmium, mainly used in batteries and the coating and plating industry, could result in stomach pains, bone fracture, possible infertility as well as serious damages to the central nervous and immune systems [2]. High ingested amounts of copper could increase infection frequencies, cardiovascular risks, and alterations in cholesterol metabolism [3]. The removal of these pollutants from industrial wastewater before discharge into the environment is, therefore, an urgent task to be appropriately achieved.

Many technologies have been developed for heavy metal removal from industrial effluents. They include chemical precipitation, reduction, electrodialysis, and membrane

separation [4–7]. These technologies have shown interesting removal efficiencies at laboratory scale. However, their upscaling to real cases has been hindered by several limitations such as high capital and exploitation costs, very sensitive operational conditions, the use of large amounts of chemicals, and the production of secondary sludge that has to be sustainably handled [7].

The adsorption technique has been pointed out as a promising, eco-friendly and low-cost method for heavy metal removal from aqueous solutions [8–12]. In general, adsorbents with high pH, important specific surface area, well developed microporosity and that are rich in specific functional groups are used for the efficient removal of heavy metals from effluents. Once the adsorption process is completed, the loaded-adsorbents could be regenerated and heavy metals could be recovered for a further subsequent use with respect to the circular economy and sustainable development concepts [13,14]. Various mineral and organic materials have been tested for Cd(II) and Cu(II) removal from synthetic/real wastewaters. They include powdered marble wastes [15], clays [16], lignocellulosic biomasses [17], biochars [18,19], activated carbons [20,21] etc.

Lignite, often referred as brown coal, is a sedimentary rock that is naturally formed from naturally compressed peat. It is a low cost material and available in various countries at high amounts [22]. Besides its classical use for energy generation, raw lignite has been tested for the removal of various pollutants from aqueous solutions such as phenol and chlorophenol [23], trichloroethylene [24], phosphorus [25] and ammonium [26]. A special focus has been dedicated to the use of these raw materials as efficient adsorbents for heavy metals from aqueous solutions [27–30]. As such, these materials have relatively high contents of functional groups such as carboxyl, alcoholic and carbonyl groups that could complex with metal ions [27,31]. Furthermore, they have a large cation exchange capacity allowing cationic pollutants to be adsorbed [32].

Laboratory investigations regarding heavy metal removal by raw lignite have demonstrated that it could be considered as an interesting candidate for single metal removal from aqueous solutions [27,30,32]. However, when in multicomponent systems, the competition phenomenon decreases their maximal adsorption capacities. In both systems, results are sometimes contradictory and highlight that the ability of heavy metal retention depends on their physico-chemical characteristics as well as the lignite properties [33,34]. For instance, Pehlivan et al. [34] studied the adsorption of Pb, Cd, Cu, Ni, and Zn on several Turkish lignite materials. They showed that the order of metal adsorption ability depends on the lignite type. However, Pb and Cu were the most adsorbed components in contrast to Ni and Zn. Furthermore, Pentari et al. [30] studied the removal of Pb, Cd, Zn, and Cu from aqueous solutions by a lignite from Greece. They found that in single mode, the ability adsorption order was as follows: $Pb > Cd > Cu > Zn$. In a multicomponent system, they showed that Cu sorption was the most affected, while Zn adsorption capacity remained quasi-constant. For the same metals in a multicomponent system, Doskočil and Pekař [33] found a different order: $Pb > Cu > Zn > Cd$. On the other hand, the involved mechanisms during heavy metal adsorption onto raw lignite are still not well identified. An in-depth kinetic and isothermal modeling study combined with lignite analysis before and after metal adsorption by using advanced techniques could reduce this gap.

As a consequence, the principal objectives of this work were: (i) to assess the adsorption characteristics of Cd and Cu onto a Tunisian lignite under various experimental conditions including contact time, initial concentration, pH, adsorbent dosage, and competition with other metals, (ii) to compare the efficiency of this lignite with raw and modified lignite available in the literature, (iii) to better understand the involved adsorption mechanisms of Cd and Cu through the combination of an in-depth modeling study and various physico-chemical analyses.

2. Materials and Methods

2.1. Adsorbent Preparation and Characterization

Raw lignite was collected from the Cap Bon region (northeastern part of Tunisia). This lignite was used in its natural state after a drying step at 60 °C for 24 h followed by manual grinding in ceramic grinder. The fraction with diameter size lower than 63 µm was selected for the adsorption tests. The preliminary characterization of the used lignite included the determination of its: (i) mineral composition by X-ray fluorescence spectrophotometer (Philips, Eindhoven, The Netherlands), (ii) Brunauer–Emmett–Teller BET specific surface area through N₂ gas adsorption method using a gas adsorption analyzer (Quantachrom Autosorb 1 sorptiometr), and (iii) pH of zero-point-charge value (pH_{ZPC}) [35].

Furthermore, advanced analyses of the lignite before and after metals adsorption were performed for a better identification of the involved mechanisms. They included the assessment of: (i) the morphology and qualitative composition through scanning electron microscopy (SEM) coupled with energy dispersive X-ray (EDX) (Philips model FEI model Quanta 400 apparatus, Amsterdam, The Netherlands), (ii) proximate analysis using a TGA/DSC3+ device (Mettler-Toledo, Greifense, Switzerland), and (iii) the existing functional groups through a Fourier transform infrared (FTIR) analysis using an Equinox 55 spectrometer (Bruker, Billerica, MA, USA). The FTIR spectra were assessed between 4000 and 400 cm⁻¹ with a resolution of 1 cm⁻¹. Experimental protocols for the above-cited analyses have already been detailed in a previous paper [36].

2.2. Synthetic Heavy Metals Solutions Preparation and Analysis

Cadmium nitrate (Cd(NO₃)₂), copper nitrate (Cu(NO₃)₂), lead nitrate (Pb(NO₃)₂), and zinc nitrate (Zn(NO₃)₂) were used for the preparation of four stock solutions at a concentration of 1 g L⁻¹ each (Fisher Scientific, Waltham, MA, USA). These solutions were used throughout this study for the preparation of adsorption solutions at precise concentrations. Metal concentrations were measured thorough an atomic absorption spectrometer (AAS) with an air-acetylene flame (Perkin Elmer Analyst 200, Waltham, MA, USA). The wavelengths used for the analysis of the Cd, Cu, Pb and Zn were 228.8, 324.8, 283.3, and 213.9 nm, respectively. The initial pH values of the solutions were adjusted by using dilute sodium hydroxide or nitric acid.

2.3. Batch Adsorption Investigation

Cd and Cu removal efficiency from aqueous solutions by raw lignite was carried under static conditions (batch mode). It consists in shaking, at room temperature (20 ± 2 °C), a given mass of lignite in 50 mL of aqueous solution containing the metal at a fixed concentration for a desired contact time at 400 rpm by using a Variomag-poly15 magnetic stirrer. Then, the suspension was filtrated through 0.45 µm cellulose acetate filter before analysis with AAS. During this study, the effect of the following experimental conditions on Cd and Cu removal efficiency were assessed: (i) particle size distribution for four lignite granulometries: <63 µm; between 63 and 500 µm; 500–1000 µm, and 1000–2000 µm; (ii) the contact time of 1; 5; 10; 20; 40; 60, and 90 min; (iii) the initial aqueous pH for 2.0; 3.0; 4.0 and 5.0, and (iv) lignite dosages for 0.4; 1.0; 1.6; 2.0; 2.4; 3; 3.5 and 4.0 g L⁻¹. During these assays, the default following parameters were used: a lignite size fraction lower than 63 µm, a contact time of 90 min, an initial Cd or Cu concentration of 100 mg L⁻¹, an initial pH of 5 and a lignite dosage equal to 2 g L⁻¹. Finally, the competing effect was determined for a multicomponent solution containing Cd, Cu, Pb and Zn at constant concentrations of 30 mg L⁻¹. All these experiments were carried out in triplicate and mean values are reported in this work. The standard deviation for all assays was lower than 5%.

The adsorbed metal amount at a given moment '*t*', (*q_t*) and the related removal yield (*Y_t*) were determined as follows [37]:

$$q_t = \frac{(C_0 - C_t)}{D} \quad (1)$$

$$Y_e(\%) = \frac{(C_0 - C_t)}{C_0} \times 100 \quad (2)$$

where C_0 and C_t (mg L^{-1}) are initial metal concentrations and at a given time ' t ', respectively, and D is the used adsorbent dose (g L^{-1}).

Cadmium and copper adsorption kinetics were fitted to three standard models namely, pseudo-first order (PFO), pseudo-second order (PSO), and intraparticle and film diffusion. Moreover, the experimental isothermal data were fitted to Langmuir, Freundlich and Dubinin–Radushkevich (D-R) isotherm models. The agreement between the experimental and theoretical adsorbed amounts was assessed through the determination of the average percentage errors (*APE kinetic* and *APE isotherm*) as follows:

$$APE_{kinetic}(\%) = \frac{\sum |(q_{t,exp} - q_{t,theo}) / q_{t,exp}|}{N} \times 100 \quad (3)$$

$$APE_{isotherm}(\%) = \frac{\sum |(q_{e,exp} - q_{e,theo}) / q_{e,exp}|}{N} \times 100 \quad (4)$$

where $q_{t,exp}$ and $q_{t,theo}$ (mg g^{-1}) are the experimental and the theoretical adsorbed amounts at a given time ' t '; $q_{e,exp}$ and $q_{e,theo}$ (mg g^{-1}) are the experimental and the theoretical adsorbed masses at equilibrium.

3. Results

3.1. Lignite Characterization

The XRF analysis of the lignite showed that it contains various minerals. Silica, Sulfur, iron, and aluminum exist at relatively high contents of 6.2%, 5.1%, 2.6%, and 2.5% (dry mass), respectively. Lower contents of 0.06%, 0.46%, 1.21%, and 0.21% were observed for Na, K, Ca, and Mg, respectively. Some of these elements could be exchanged with Pb(II) during its adsorption by lignite. On the other hand, the used material has higher concentrations of Si, Al, Fe and Na and lower Ca and Mg content than a commercial and natural lignite from Czech Republic [38,39]. The BET surface area of the lignite was assessed to $11.2 \text{ m}^2 \text{ g}^{-1}$, which is in the range of BET values reported for Greek lignites (between 3.6 and $23.8 \text{ m}^2 \text{ g}^{-1}$) [30]. For instance, it is about 12-fold higher than a lignite from Poland ($0.91 \text{ m}^2 \text{ g}^{-1}$) [23], and about two-fold higher than a Hungarian lignite ($5.3 \text{ m}^2 \text{ g}^{-1}$) [25]. This relatively higher surface area suggests that the used lignite could exhibit more metal adsorption capacities compared to other lignites reported in the literature. On the other hand, its pH_{ZPC} was estimated to 3.6. It is lower than that of a Czech lignite (5.0) [38], and a Polish lignite (6.2) [23]. In contrast, it is higher than pH_{ZPC} of a Hungarian lignite (2.6) [25]. Since the net charge surface of the adsorbent becomes negative for aqueous pH values higher than pH_{ZPC} , the removal of positively charged metals by the current lignite through electrostatic attraction will be favored for a wide pH range.

3.2. Batch Adsorption Results

3.2.1. Effect of Lignite Granulometry

The impact of lignite granulometry on Cd and Cu removal from the synthetic solution was carried out for initial metal concentrations of 100 mg L^{-1} each, initial pH of 5 and a dosage of 2 g L^{-1} . The experimental results (Figure 1) showed that coarser is the lignite fraction, lower is Cd or Cu removal efficiency. Accordingly, the highest adsorbed amounts of Cd (26.1 mg g^{-1}) and Cu (18.6 mg g^{-1}) were observed for the finest granulometry ($<63 \mu\text{m}$). These adsorbed Cd and Cu amounts decreased by about 25% and more than 65%, respectively when lignite particles of 1–2 mm size were used. This outcome could be attributed to the lower microporosity and surface area generally observed for coarser media [40]. Similar behavior was observed by PN and CP [41] when investigating an oily effluent treatment by hard wood based adsorbents. They reported a decrease of the removal efficiency by about 30% when the average size particles were increased from 0.8 to 3.5 mm.

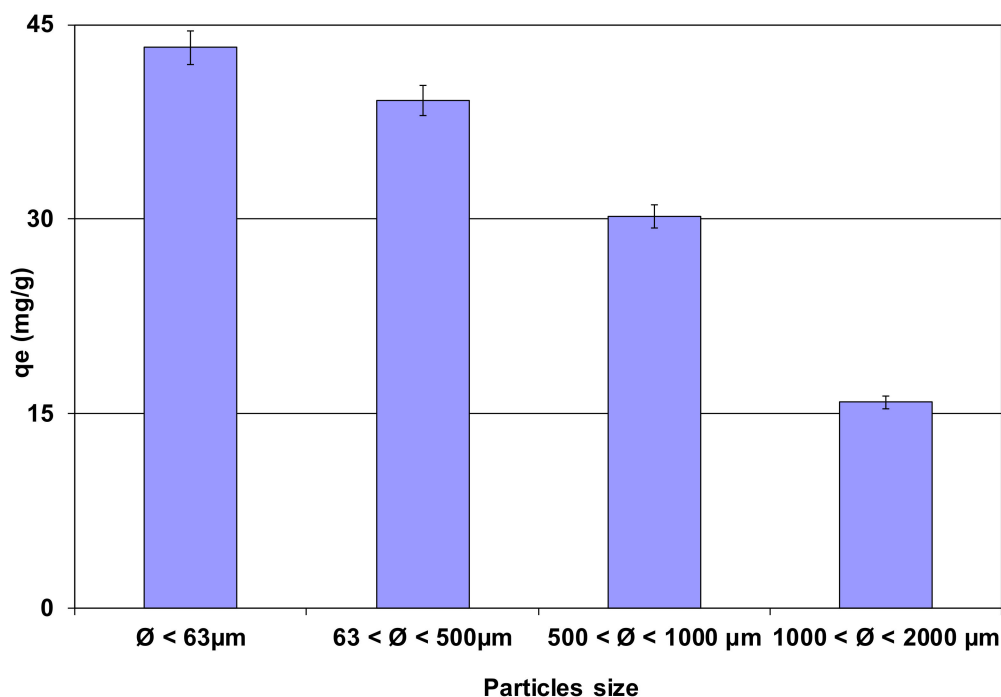


Figure 1. Impact of lignite particle size on Cd and Cu removal efficiency ($C_0 = 100 \text{ mg L}^{-1}$, $D = 2 \text{ g L}^{-1}$; $t = 60 \text{ min}$; $\text{pH} = 5$; $T = 20 \pm 2 \text{ }^\circ\text{C}$).

3.2.2. Effect of Contact Time—Kinetic Study

The removal of Cd and Cu by the used lignite is clearly a time-dependent process as shown in Figure 2. Indeed, their removal was very rapid at the beginning of the adsorption (especially for Cd) since about 78% and 44% of the totally removed amounts were adsorbed after only 1 min for Cd and Cu, respectively. This finding suggests that Cd removal occurs mainly through surface reactions [11]. The high reactivity of the used lignite could result in an important energy saving when such process is scaled up for field investigations. After this contact period, the adsorbed amounts continue to increase but at much slower rate. This behavior is linked to an intraparticle diffusion inside the pores of the lignite and adsorption by functional groups through complexation process [42]. The equilibrium state which corresponds to quasi-constant adsorbed amounts was reached after approximately 60 min for both metals. This time is 6-fold lower than the one reported by Havelcova et al. [38] when investigating Cd, Cu and Zn removal by a local lignite from south Moravian coal field (Czech republic) and 12-fold lower than the duration observed by Pentari et al. [43] for Cd removal by a raw and iron doped Greek lignite. However, relatively similar equilibrium contact times were observed for Cd and Cu removal by various Greek lignites [30]; Cu, Pb and Ni removal by two Turkish lignites [32]; Zn removal by a commercial lignite from South Korea [44] and Cr(VI) adsorption onto a raw Iranian lignite [28]. For economic reasons, low contact times, ensuring percentages removal of more than 80% of the totally adsorbed Cd or Cu amounts could be used in real case application. These durations correspond to only 5 and 20 min for Cd and Cu, respectively.

At equilibrium, the lignite sample used in this study removed Cd better than Cu. Indeed, the adsorbed Cd amount by was assessed to 26.1 mg g^{-1} which is about 41% higher than Cu (Figure 2). A Similar trend was observed by various studies dealing with heavy metal adsorption onto lignite [30,38]. This behavior is mainly imputed to their physico-chemical properties, especially electronegativity, ionic potential and ionic radius [45].

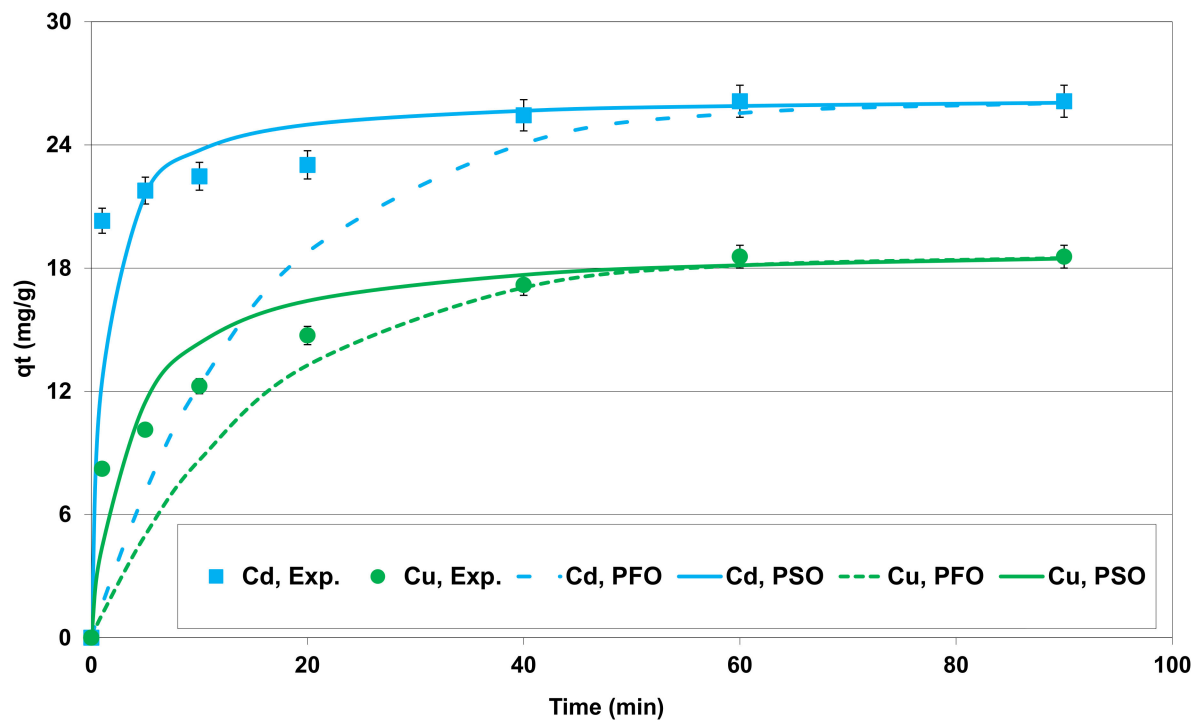


Figure 2. Kinetics of Cd and Cu removal by lignite and its fitting with PFO and PSO models ($C_0 = 100 \text{ mg L}^{-1}$, $D = 2 \text{ g L}^{-1}$; $t = 60 \text{ min}$; $\text{pH} = 5$; $T = 20 \pm 2 \text{ }^\circ\text{C}$; Exp.: Experimental value).

The parameters of the three theoretical models: PFO, PSO and diffusion models are given in Table 1. Based on these calculated parameters, it can be clearly deduced that the PFO model does not appropriately fit to the experimental data. In fact, the corresponding determination coefficients were low: 0.553 and 0.883 for Cd and Cu, respectively. The calculated APE between the measured and calculated adsorbed masses were high since they are about 28% for Cd and 22% for Cu. Figure 2 confirms this finding since the dashed lines are far from the measured data.

Table 1. Kinetic parameters of Cd and Cu removal by the used lignite ($C_0 = 100 \text{ mg L}^{-1}$, $D = 2 \text{ g L}^{-1}$; $t = 60 \text{ min}$; $\text{pH} = 5$; $T = 20 \pm 2 \text{ }^\circ\text{C}$).

	Cadmium	Copper
$q_{e,\text{exp}} \text{ (mg g}^{-1}\text{)}$	26.1	18.6
Pseudo-first-order-model (PFO)		
$k_1 \text{ (min}^{-1}\text{)}$	0.063	0.063
R^2	0.533	0.883
APE (%)	28.9	22.5
Pseudo-second-order-model (PSO)		
$q_{e,\text{theo}} \text{ (mg g}^{-1}\text{)}$	26.4	19.2
$K_2 \text{ (g mg}^{-1} \text{ min}^{-1}\text{)}$	0.034	0.016
R^2	0.894	0.932
APE (%)	6.9	11.7
Diffusion model		
$D_f \text{ (}\times 10^{-14} \text{ m}^2 \text{ s}^{-1}\text{)}$	4.68	2.04
R^2	0.750	0.844
$D_{ip} \text{ (}\times 10^{-14} \text{ m}^2 \text{ s}^{-1}\text{)}$	2.26	2.16
R^2	0.936	0.999

In contrast, the PSO model fits well the experimental data for both metals. The related determination coefficients (>0.89) were much higher than those for the PFO model. Furthermore, the APE for Cd and Cu were determined to only 7% and 12% for Cd and Cu, respectively and therefore were lower than those obtained for the PSO model. The theoretical adsorbed amounts of Cd and Cu at equilibrium ($q_{e,theo}$), were very close to the experimental ones (Figure 2 and Table 1), with different percentages of about 1% and 3%, respectively. Therefore, under the used experimental conditions, the PSO model is more suitable in fitting the Cd and Cu removal onto lignite. This model suggests that the rate limiting step might be chemical adsorption involving valency forces through sharing or exchange of electrons between these two metals and lignite [46].

The analysis of the adsorption of Cd and Cu onto the used raw lignite through the application of film and intraparticle diffusion models indicated clearly that the adsorption process proceeds by surface interactions at earlier stages (short times, less than 5 min) and by intraparticle diffusion at later stages (Figure 2). For Cd, the film diffusion coefficient (through boundary layer) is about two times higher than the one of the intraparticle diffusion. This explains the very high adsorption percentage observed after only 1 min (Figure 2). This finding confirms that intraparticle diffusion process controls significantly the rate of Cd adsorption onto the lignite. Similar observations were reported by Pehlivan et al. [32] when studying Pb, Cu, Ni, and Zn removal by Turkish lignites. For Cu, the film and intraparticle diffusion coefficients are quite similar (Table 1) indicating that both processes (boundary layer and intraparticle diffusion) control its removal by the raw lignite.

3.2.3. Effect of Initial Aqueous pH

The effect of the initial aqueous pH on Cd and Cu removal efficiency was performed under the experimental conditions presented in Section 2.3. The experimental results showed that for both metals, the removed amounts increased with the increase of the aqueous pH (Figure 3). As such, for an initial pH of 2, the adsorbed amounts of Cd and Cu were 10.9 and 5.4 mg g⁻¹, respectively. At a pH of 5, these quantities reached 26.1 and 18.6 mg g⁻¹ which are about 2.4 and 3.4 times higher than those registered at an initial pH of 2. This outcome could be explained by the lignite surface charge that is positive at aqueous pH lower than the pH_{ZPC} (3.6), which will repulse the two cationic metals. Furthermore, at this pH range, abundant H⁺ ions in the solution will compete with Cd and Cu over the adsorption sites. However, when the used aqueous pH value is higher than the pH_{ZPC} , the lignite surface will carry more negative charges and will consequently favor Cd and Cu adsorption through electrostatic reactions. At this pH range, H⁺ and other exchangeable cations such as Ca²⁺, Mg²⁺, Na⁺, and K⁺ could be exchanged with these metals and released in the aqueous solutions. Similar trends were reported by several studies dealing with heavy metals or cationic pollutant adsorption onto raw or modified lignites [32,38] and other adsorbents [35,42,47,48]. For instance, Pehlivan et al. [32] showed that increasing pH from 2 to 6 increased Cu removal efficiency yield by a raw Turkish lignite from about 8% to more than 88%.

3.2.4. Effect of Lignite Dosage

The impact of lignite dose on Cd and Cu removal from aqueous solutions at an initial concentration of 100 mg L⁻¹, an initial pH of 5 and 60 min of contact time is given in Figure 4. Their removal yields increase with the increase of the lignite dose. As such, rising the dose from 0.4 to 3 g L⁻¹, Cd and Cu removal efficiencies increased from about 40.5% and 19.8% to 61.9% and 46.7%, respectively. This important increase is linked to the presence of more available adsorption sites that could interact with Cd or Cu when using higher doses. Starting from a used dose of 3.5 g L⁻¹, Cd or Cu removal efficiency remains approximately constant due to the saturation of lignite particles. Such high removal efficiencies observed for relatively low lignite doses is a real asset for larger applications at industrial levels.

A similar trend was reported by Binabaj and Ramezani [28] and Gurses et al. [49] when studying chromium(VI) and methylene blue removal by raw lignites, respectively.

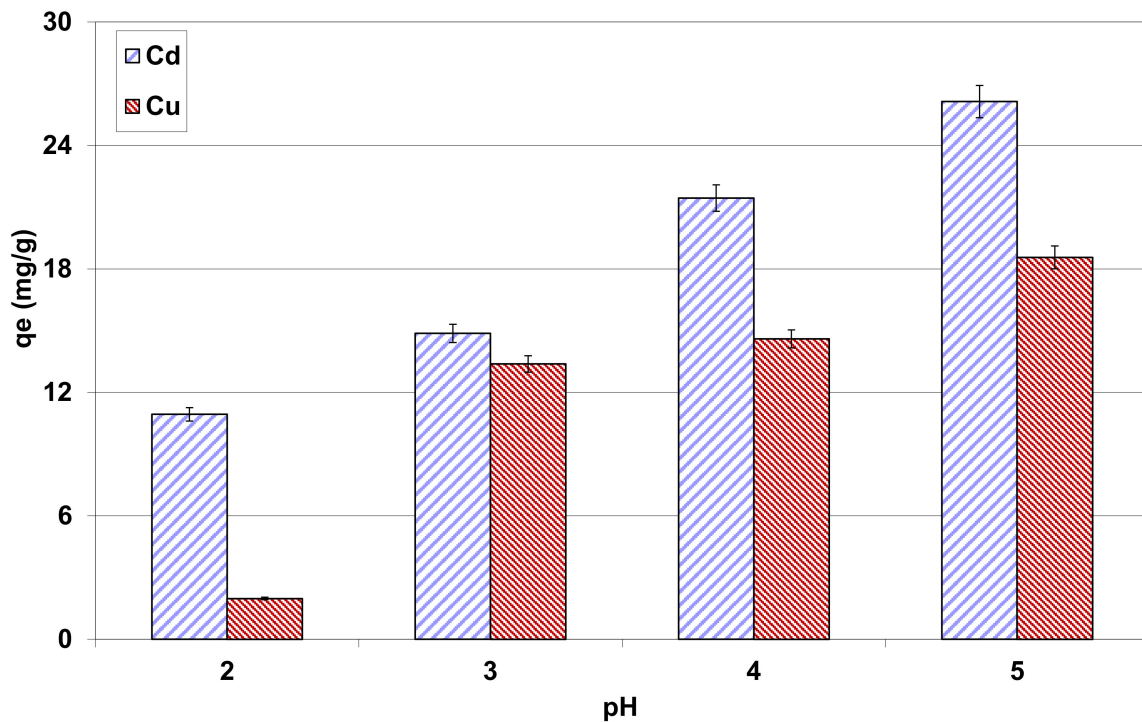


Figure 3. Impact of initial aqueous pH on Cd and Cu removal efficiency by lignite ($C_0 = 100 \text{ mg L}^{-1}$, $D = 2 \text{ g L}^{-1}$; $t = 60 \text{ min}$; $T = 20 \pm 2 \text{ }^\circ\text{C}$).

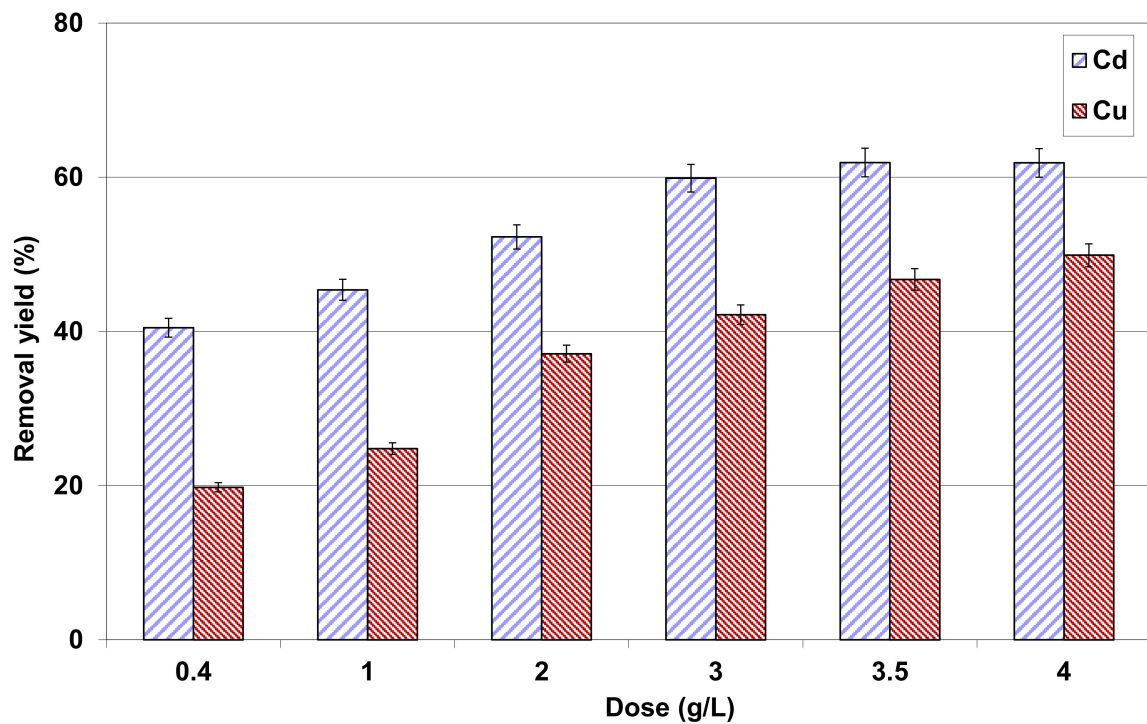


Figure 4. Impact of lignite dose on Cd and Cu removal yields ($C_0 = 100 \text{ mg L}^{-1}$, $t = 60 \text{ min}$; $\text{pH} = 5$; $T = 20 \pm 2 \text{ }^\circ\text{C}$).

3.2.5. Competing Effect

Industrial effluents generally contain a complex mixture of organic and non-organic pollutants. The effect of the presence of Pb and Zn on the adsorption of Cd and Cu by the raw lignite was performed according to the experimental conditions described in Section 2.3. The experimental results (Figure 5) showed that for single mode, as reported by Pentari et al. [30], the adsorption efficiency of the studied metals was as follows: Pb > Cd > Cu > Zn. The corresponding removal percentages were estimated at 100%, 74.6%, 71.7% and 44.8%, respectively. Similar observations were also reported by Pehlivan et al. [34] who studied the adsorption of Pb, Cd, Cu, Ni, and Zn on several Turkish lignites. They showed that for the majority of the studied lignites, Pb, Cu and Cd were the most adsorbed metals whereas Ni and Zn were the less adsorbed ones.

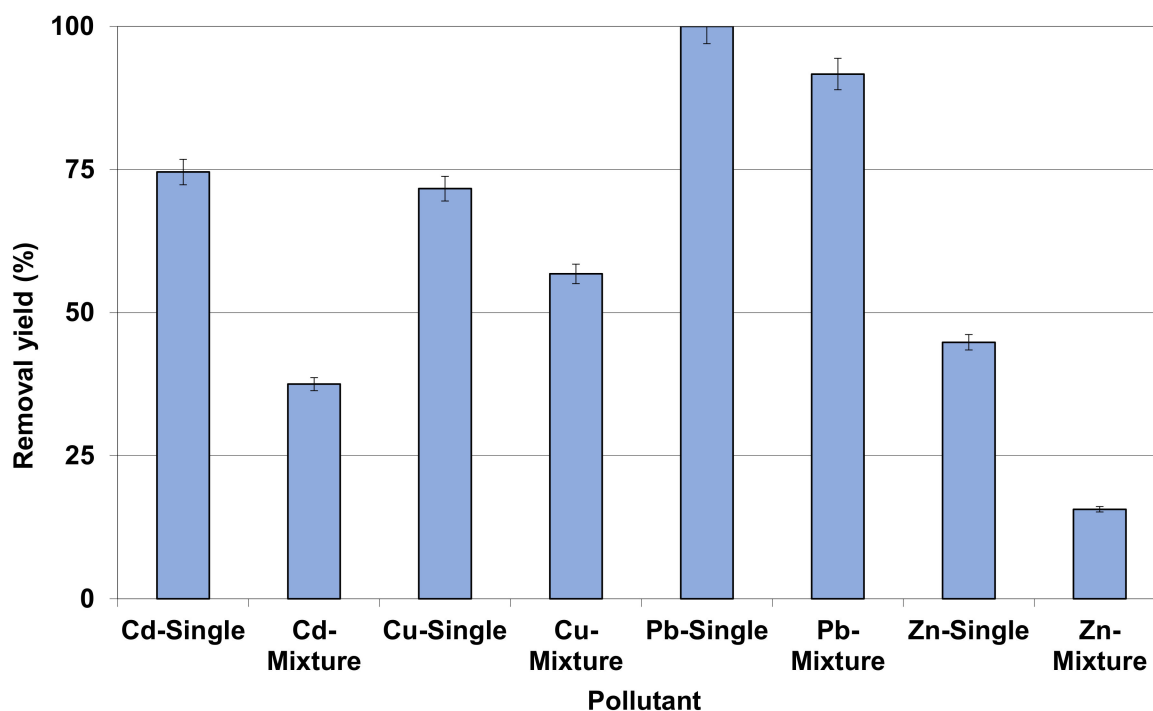


Figure 5. Cd, Cu, Pb and Zn removal yield in single and multicomponent systems ($C_0 = 30 \text{ mg L}^{-1}$ for all metals; $D = 2 \text{ g L}^{-1}$; $t = 60 \text{ min}$; $\text{pH} = 5$; $T = 20 \pm 2 \text{ }^\circ\text{C}$).

In the multicomponent system, all the removal efficiencies of the four heavy metals significantly decreased due to competition. Accordingly, the highest removal decrease was observed for Cd (37.1%) and Zn (29.2%) and the adsorption pattern shifted to: Pb > Cu > Cd > Zn with removal efficiencies of 91.7%, 56.8%, 37.5% and 15.6%, respectively. Consequently, when treating real wastewater containing a mixture of heavy metals, Pb and Cu will be favorably retained by the current lignite compared to other metals. Similar trends were reported by Allen and Brown [50] when investigating the removal of Cd, Cu and Zn by an Irish lignite in a single and multicomponent systems. Their experimental results showed that in single metal sorption mode, the adsorption ability decreases in the order Cd > Cu > Zn. However, in the multicomponent assays, this order changed to: Cu > Cd > Zn. This result is in a contradiction with the one reported by Pentari et al. [30] who pointed out that in multicomponent system containing Pb, Cd, Cu, and Zn, copper adsorption was the most significantly influenced by the presence of the other elements with a total yield reduction of about 5%. This behavior should not be only attributed to metal characteristics including size, electronegativity, availability and hydration energy [15] but also to the physico-chemical properties of the lignite such as the donor atoms abundance (oxygen, nitrogen, sulphur [51]).

3.2.6. Isotherm Adsorption

For the experimental conditions cited in Section 2.3, the data of Cd and Cu adsorption isotherms in comparison with the predicted ones using Freundlich, Langmuir and D-R models are given in Figure 6. Table 2 gives the parameters of these models as well as their fitness to the experimental data.

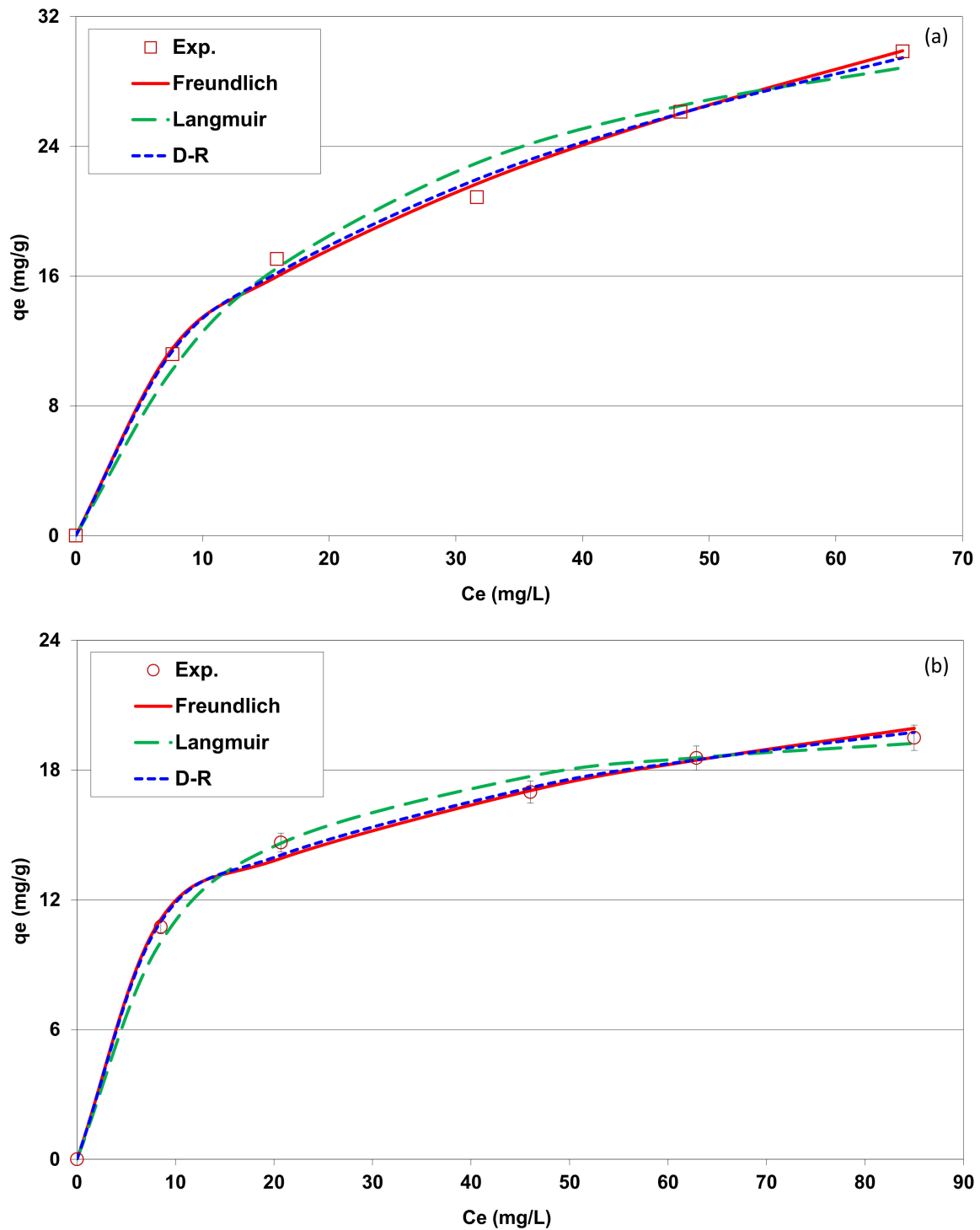


Figure 6. Isotherm experimental and fitted data with Freundlich, Langmuir and Dubinin–Radushkevich (D-R) models for Cd (a) and Cu (b) removal by lignite ($D = 2 \text{ g L}^{-1}$; $t = 60 \text{ min}$; $\text{pH} = 5$; $T = 20 \pm 2 \text{ }^\circ\text{C}$; Exp.: Experimental value).

Table 2. Adsorption isotherm parameters of Cd and Cu removal by lignite ($D = 2 \text{ g L}^{-1}$; $t = 60 \text{ min}$; $\text{pH} = 5$; $T = 20 \pm 2 \text{ }^\circ\text{C}$).

Metal	Cd	Cu
Freundlich model		
Freundlich constant: K_F	4.7	6.4
Freundlich constant: n	2.3	3.9
Determination coefficient: R^2	0.991	0.983
Average percentage error: APE (%)	2.8	2.3
Langmuir model		
Langmuir's maximum adsorption capacity; q_m (mg g^{-1})	38.0	21.4
Langmuir constant: K_L	0.048	0.104
Determination coefficient: R^2	0.979	0.957
APE (%)	5.4	2.5
D-R model		
DR's maximum adsorption capacity; q_m (mg g^{-1})	124.8	40.5
E (kJ mol^{-1})	10.7	13.4
Determination coefficient: R^2	0.990	0.990
APE (%)	2.3	1.5

It can be clearly demonstrated from Figure 6 and Table 2 that the three applied models fit very well with the experimental data. Nevertheless, the highest determination coefficients (R^2) (0.990 for Cd and for Cu) and the lowest APE (2.3% for Cd and 1.5% for Cu) were observed for D-R model. This model predicts, however, very high adsorption capacities for both Cd and Cu with respective values of 124.8 and 40.5 mg g^{-1} , respectively. These values are unrealistic considering the isotherm curves shape (Figure 6) and are mainly imputed to this model's used assumptions especially the one related to the uniformity and homogeneity of the adsorbent's microporous structure [35]. The calculated free energy ($E = 1/\sqrt{2\beta}$) was assessed to 10.7 and 13.4 kJ mol^{-1} for Cd and Cu, respectively. Both of them are higher than 8 kJ mol^{-1} , indicating that Cd and Cu removal by the used lignite was mainly chemical [49]. It is worth mentioning that compared to Langmuir model, The Freundlich one fits better the experimental data with higher R^2 coefficients and lower APE values (Table 2). This outcome indicates that both Cd and Cu adsorption by the used lignite occurs heterogeneously on multilayer surfaces through chemical processes [28].

On the other hand, the Freundlich constant 'n' values were 2.3 and 3.9 for Cd and Cu, respectively. They are in the range of 1–10, which indicates that the adsorption of these two heavy metals by the used lignite is a favorable process. Values in the same range were determined by Pentari et al. [30] when studying Cd and Cu removal by a raw Greek lignite. Moreover, the highest Langmuir's parameter values (obtained for the lowest used initial concentrations) ' $R_L = \frac{1}{1+K_L \cdot C_0}$ ' were estimated to 0.41 and 0.24 for Cd and Cu, respectively. They are lower than 1, suggesting that lignite could be considered as a favorable material for Cd and Cu retention from aqueous solutions.

The Langmuir's maximum adsorption capacities of Cd and Cu were determined to 38.0 and 21.4 mg g^{-1} , respectively. A comparison of the used lignite efficiency in removing Cd and Cu with other lignites (Table 3) clearly shows that it can be considered as a promising medium for the removal of heavy metals from wastewater. As a matter of fact, its Cd adsorption capacity was about 5.6, 1.7 and 1.5 times higher than a lignite activated carbon from China [52], a HNO_3 treated lignite activated carbon [52], and a raw lignite from Greece [43]. Its Cu adsorption capacity was higher than a Beypazari lignite [51], Ilgin lignite and Beysehir lignite [32]. However, other tested lignites exhibited higher adsorption capacities [27,30,53]. It is important to underline that the observed lignite adsorption capacities of Cd and Cu are also higher than various other agricultural, animal and industrial wastes [54,55]. As compared to natural agricultural wastes, Cd adsorption capacity of the studied lignite was about 7.5 and 2.3 higher than corn cob [56] and rice

husk [57], respectively. Moreover, Cu removal was 2.8 and 2.1 times more important than Banana peels [58] and grape stalks [59], respectively.

Table 3. Comparison of the used lignite removal efficiency of Cd and Cu with other lignites from various regions.

Material	BET Surface Area (m ² g ⁻¹)	Adsorption Conditions	Cd Langmuir Adsorption Capacity (mg g ⁻¹)	Cu Langmuir Adsorption Capacity (mg g ⁻¹)	Reference
Lignite, Beypazarı, Turkey	2.56	C ₀ = 0.00015–0.0015 M; pH = 4; D = 10 g L ⁻¹ ; t = 1 h; T = 20 °C	-	1.62	[51]
Ilgin lignite, Konya, Turkey	2.06	C ₀ = 0.0025–0.025 M; pH = 4.5; D = 4 g L ⁻¹ ; t = 120 min; T = 20 °C	-	17.8	[32]
Beysehir lignite, Konya, Turkey	2.96		-	18.9	
Tyul'gansk lignite, South Ural Basin Russia	-	C ₀ = 0.1 M; pH = 4.1; D = 40 g L ⁻¹ ; t = 5 days; T = 25 °C	-	27.3	[27]
Tisul'sk lignite, Kansk-Achinsk Basin, Russia	-		-	27.3	
Lignite, South Moravian deposit, Mikulcice, Czech Republic	-	C ₀ = 0.001–0.2 M; pH = 4–5; D = 20 g L ⁻¹ ; t = 24 h; T = 25 °C	-	82.0	[53]
Lignite activated carbon (LAC), China	158.11	C ₀ = 0.00015–0.0015 M; pH = 7.2; D = 1 g L ⁻¹ ; t = 24 h; T = 25 °C	6.8	-	[52]
Lignite activated carbon, treated with sodium dodecyl benzene sulfonate (SAC)	118.2		26.6	-	
HNO ₃ -treated lignite activated carbon (NAC)	185.07		22.8	-	
HNO ₃ -treated lignite activated carbon, post treated with sodium dodecyl benzene sulfonate (NSAC)	131.4		44.2	-	
Lignite, Drama, northern Greece	154	C ₀ = 0.00015–0.015 M; pH = 4.5; D = 10 g L ⁻¹ ; t = 12 h; T = 25 °C	25.5	-	[43]
Same lignite doped with Nano-scale-zero-valent-iron particles	109		34.7	-	
Lignite, Macedonia and Thrace, Greece	4.2	C ₀ = 0.00015–0.015 M; pH = 4–5; D = 10 g L ⁻¹ ; t = 45 min; T = 25 °C	51.5	42.7	[30]
Lignite, Cap Bon, Tunisia	11.2	C ₀ = 0.00047–0.00197 M; D = 2 g L ⁻¹ ; pH = 5; T = 20 ± 2 °C	38.0	21.0	Current study

As illustrated in Table 3, Cd or Cu adsorption efficiency by lignites depend not only on their specific surface area (case of the activated lignites [52]) but also on their functional group types and richness and the experimental conditions. The same trend was reported by Puglla et al. [19] who found relatively low adsorption capacities of Cd onto biochars derived from peanut shell (1.038 mg g⁻¹), chonta pulp (0.655 mg g⁻¹) and corncob (0.857 mg g⁻¹) even if they have interesting textural properties. It is important to underline that the structural and textural properties of the lignite could be improved through specific physical/chemical/thermal modifications [52,60,61]. For instance, Sun et al. [52] found that the chemical/thermal modification of lignite by a HNO₃ solution simultaneously increased its surface area (from 158.1 to 185.1 m² g⁻¹) and its surface carboxylic and lactone functional groups (from 0.55 to 1.26 mmol g⁻¹). Consequently, such modification increased Cd removal capacity from 6.8 to 26.6 mg g⁻¹.

3.3. Raw and Metal-Loaded Lignite Characterization and Adsorption Mechanism Exploration

Various techniques were used for the characterization of lignite before and after metal adsorption in order to get a better understanding of the probably involved mechanisms. Morphological properties of the lignite before and after adsorption of metals were investigated through imagery comparison using scanning electron microscopy and energy-dispersive X-ray spectroscopy (Figures 7 and 8).

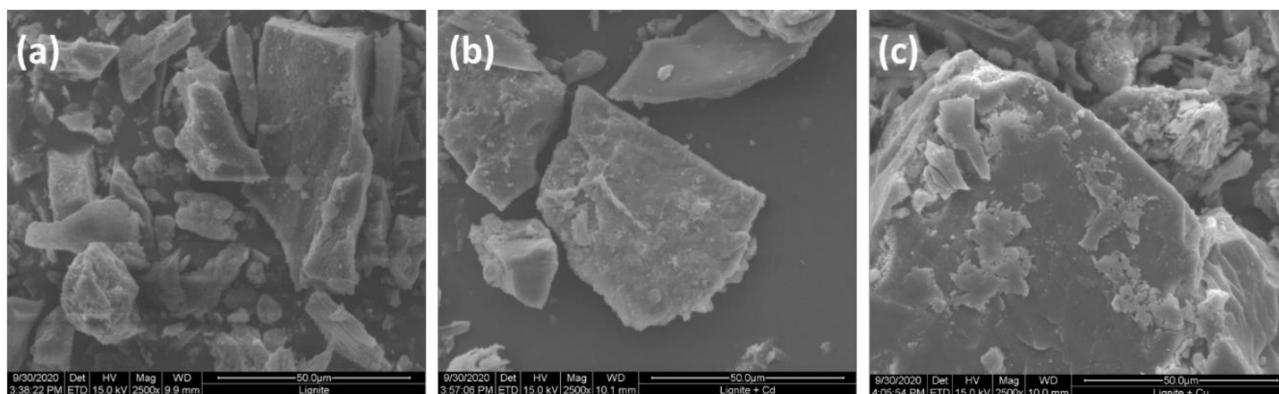


Figure 7. SEM images of: (a) raw lignite; (b) after adsorption of cadmium; (c) after adsorption of copper (magnitude: $\times 2500$).

It appears that the raw lignite (particle size lower than $63 \mu\text{m}$) presents an irregular and heterogeneous surface. Moreover, similarly to the majority of natural carbonaceous materials, the used lignite does not present a concrete porosity (Figure 7a), which explain its measured specific surface area. SEM imaging reveals also the presence of crystalline structures on the surface. According to Zhang and Chen [62], raw uncrushed lignites could present some typical cellular plant structures such as fusinites and semifusinites, intergranular and plant tissue pores along with some crystalline impurities identified mainly as calcium carbonates and silicon dioxide as well as other trace elements such as aluminum and iron ions. This was confirmed by EDX analysis where the raw material presents high peak intensities of oxygen, silica and calcium (Figure 8a). After the adsorption process, SEM images of the metal-loaded lignite presented a clearer contrast on its surface for both metals, while the crystalline structure present in the raw material became less apparent (Figure 7b,c). This observation could be due to an adsorption reaction of metals on the lignite surface and at the same time to a possible inverse movement of some minerals from lignite to the liquid phase. The EDX analysis confirmed this hypothesis since the peaks related to oxygen, silica, potassium, and calcium decreased in intensity, while peaks attributed to copper and cadmium appeared, which confirms the adsorption process (Figure 8b,c).

The proximate analysis (Figure 9) indicates that the raw lignite is mainly composed of minerals with an ash content of about 39%. Its moisture, fixed carbon and volatile matter contents are respectively 7%, 21% and 33%. Similar trends were reported by Kanca [63] for a Turkish lignite, where ash content had the major proportion (48%) followed by volatile matter and fixed carbon (25% and 24%, respectively).

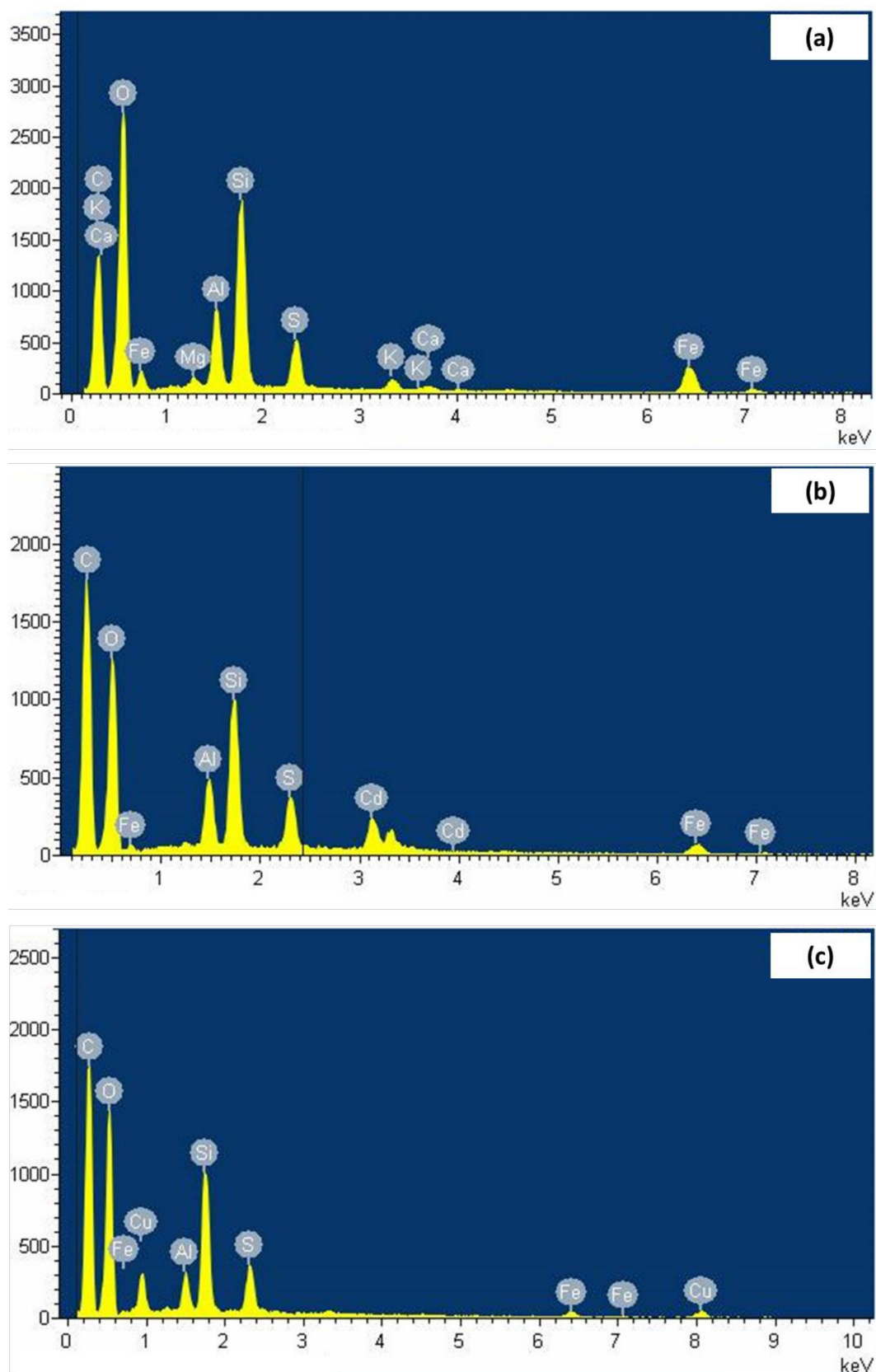


Figure 8. EDX analysis of: (a) raw lignite; (b) cadmium-loaded lignite; (c) copper-loaded lignite.

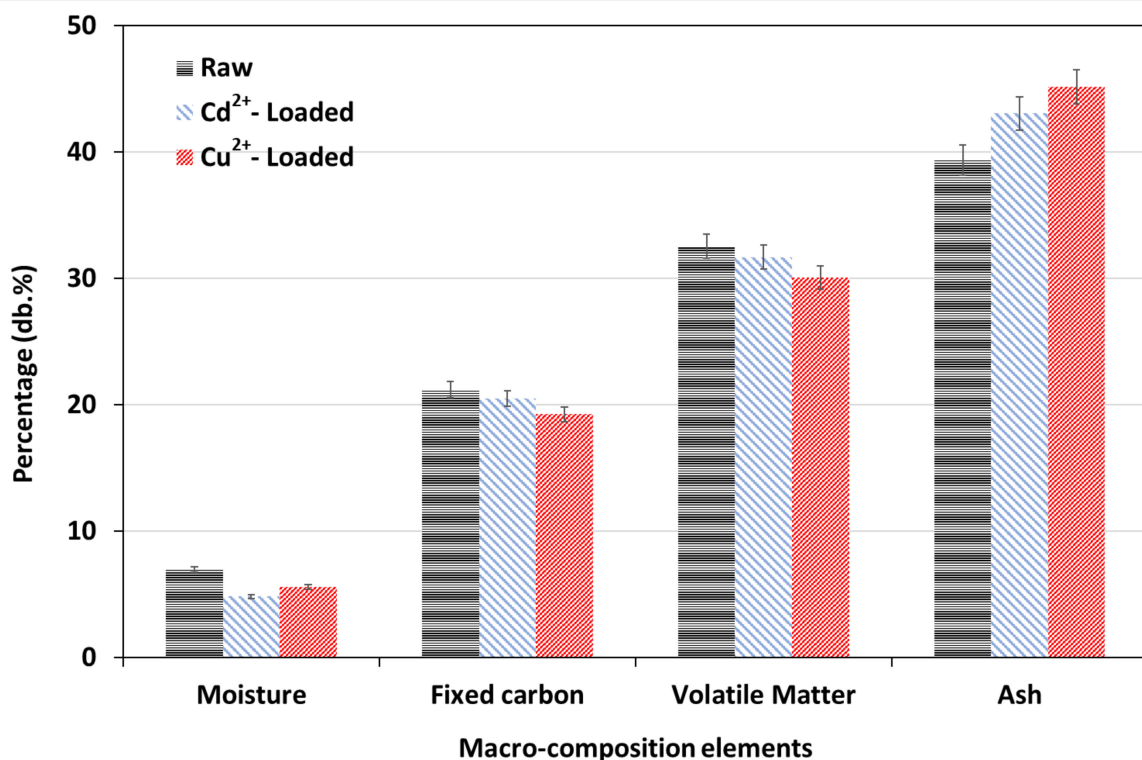


Figure 9. Proximate analysis of lignite before and after copper and cadmium adsorption.

After metal adsorption, a slight decrease of the fixed carbon and volatile matter contents occurred in favor of an ash content increase by about 3.7% and 5.8% for Cd- and Cu-loaded lignite, respectively. To align these results with SEM/EDS observations, it is possible that the adsorption of cadmium and copper were driven by three mechanisms: (i) adsorption of a small fraction of metal ions onto lignin decayed matrix which constitutes the small specific surface area of the feedstock yet characterized, (ii) ion-exchange reaction where ions such as potassium, calcium then silica at lower percentage were diffused from the solid matrix to the aqueous solution thus vacating the oxygenic functional groups, and (iii) chemical adsorption on free surface functional groups.

In order to confirm this hypothesis, FTIR analyses were performed on both raw and metal-loaded lignite and results are depicted in Figure 10 and Table 4. The lignite presented a heterogeneous surface with the co-presence of acidic and alkaline functional groups namely, hydroxyl (-OH ; $3600\text{--}3200\text{ cm}^{-1}$), aliphatic (C-H ; $3000\text{--}2700\text{ cm}^{-1}$), carbonyl and acetyl esters (C=O and C-O ; $1650\text{--}1600\text{ cm}^{-1}$ and $1180\text{--}980\text{ cm}^{-1}$, respectively), methyl and methylene aromatic ($\text{-CH}_2/\text{-CH}_3$; $1465\text{--}1320\text{ cm}^{-1}$) and out-of-plane aromatic groups (C-H ; $896\text{--}809\text{ cm}^{-1}$). After metal adsorption, few modifications were noticed for peak positions of some functional groups due to their involvement in the adsorption process (Table 4). For instance, a peak shift of about $+8$ and $+4\text{ cm}^{-1}$ was noticed for hydroxyl groups after Cd and Cu adsorption, respectively. Similar observation for carboxylic group where a vibration was spotted by about -4 and -6 cm^{-1} as compared to raw lignite for the same exhausted adsorbents, respectively. Moreover, a significant change was observed in the C=C aromatic structure where a peak appeared for both Cd- and Cu-related specters at 1382 and 1380 cm^{-1} , respectively (Table 4). This could be related to the uptake of nitrate ions (entering in the composition of copper and cadmium reagents) by the lignite matrix, causing a slight alteration in its surface functionalities [64].

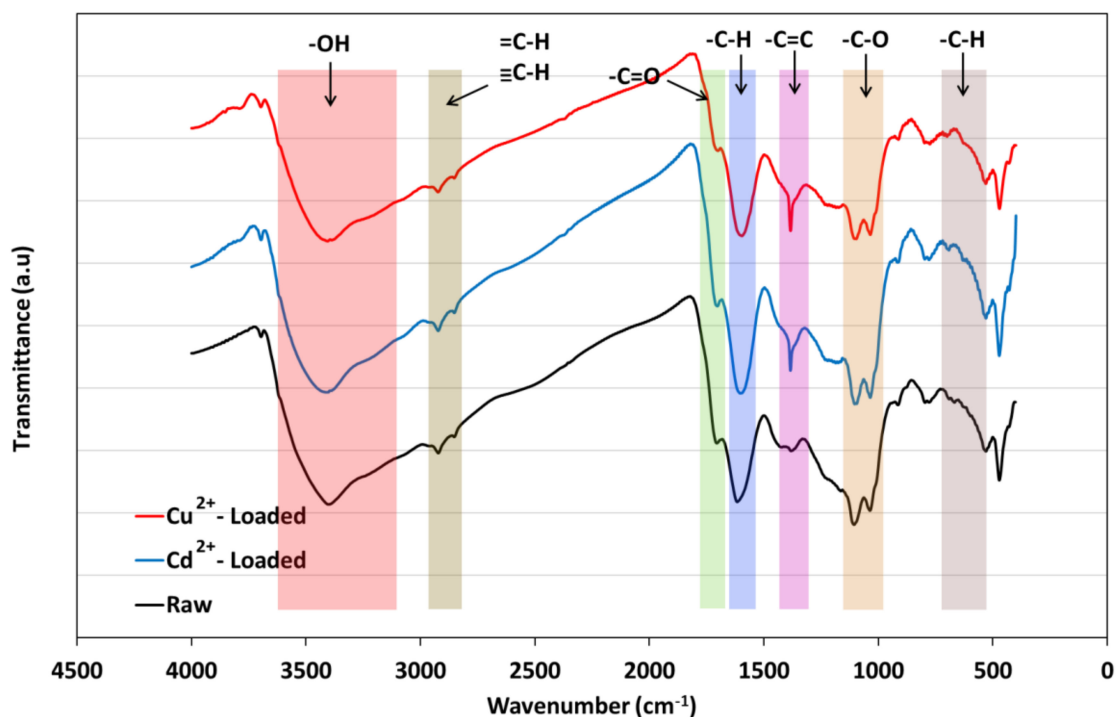
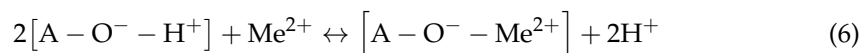


Figure 10. FTIR analysis of lignite before and after Cu (II) and Cd (II) adsorption.

Table 4. Peak location for each functional group detected in FTIR spectra for raw and metal-loaded lignite.

Functional Group	-OH	C=O	C-H	-C=C	-C-O	-C-H
Raw	3400	1705	1614	Absent	1105	794
Cd ²⁺ -loaded lignite	3408	1701	1600	1382	1101	794
Cu ²⁺ -loaded lignite	3404	1699	1593	1380	1103	794

On the other hand, the presence of positively charged metals (i.e., Cd²⁺ and Cu²⁺) caused a thermodynamic balance between solid and liquid phases. It is possible that a cation release phenomenon occurred leading to the release of protons (H⁺) or other cations (Na⁺; K⁺; Ca²⁺, and Mg²⁺) followed by the fixation of bivalent metals on the oxygenic functional groups as follows [19,65]:



where A stands for the aromatic structure of lignite and Me²⁺ is either Cu²⁺ or Cd²⁺.

On the basis of FTIR investigation, we can deduce that Cd and Cu removal by lignite is governed not only by its textural properties (especially surface area and microporosity), but also by its richness in functional groups.

4. Conclusions

The current research study demonstrates that lignite, as a low cost and abundant material, can achieve very rapid and effective removal of cadmium and copper from aqueous effluents under wide experimental conditions. The removal efficiency seems not only dependent on the heavy metal properties but also on the textural and structural characteristics

of the lignite. The heavy metal adsorption process occurs through a combination of several mechanisms, including mainly cation exchange and complexation with various functional groups. Lignite adsorption capacity could be further enhanced through physical, chemical, and thermal treatment methods. However, the cost and the environmental impact of such modifications should be accurately assessed. Moreover, further studies are required in order to assess the efficiency of raw/modified lignite for the removal of other heavy metals and recalcitrant organic pollutants under dynamic conditions.

Author Contributions: Conceptualization, S.J. and A.M.; methodology, S.J., A.M. and M.J.; validation, S.J., A.M. and A.A.A.; formal analysis, S.J., A.A.A., M.J., H.H. and A.M.; investigation, S.J. and A.M.; resources, S.J. and A.M.; writing—original draft preparation, S.J. and A.A.A.; writing—review and editing, A.M., H.H. and M.J.; visualization, S.J., A.M., A.A.A., H.H. and M.J.; supervision, S.J. and A.M.; project administration, A.M.; funding acquisition, A.M. All authors have read and agreed to the published version of the manuscript.

Funding: This research was funded by The Tunisian Ministry of Higher Education and Scientific Research.

Institutional Review Board Statement: Not applicable.

Informed Consent Statement: Not applicable.

Data Availability Statement: Data available on request.

Acknowledgments: Authors would like to thank all technicians involved in this work. The Tunisian Ministry of Higher Education and Scientific Research is gratefully acknowledged for financing this research project.

Conflicts of Interest: The authors declare no conflict of interest

References

1. Morais, S.; Costa, F.G.; Pereir, M.L. Heavy Metals and Human Health. In *Environmental Health—Emerging Issues and Practice*; IntechOpen: London, UK, 2012.
2. Sharma, H.; Rawal, N.; Mathew, B.B. The Characteristics, Toxicity and Effects of Cadmium. *Int. J. Nanotechnol. Nanosci.* **2015**, *3*, 1–9.
3. Araya, M.; Olivares, M.; Pizarro, F. Copper in human health. *Int. J. Environ. Health* **2007**, *1*, 608. [[CrossRef](#)]
4. Abdullah, N.; Yusof, N.; Lau, W.; Jaafar, J.; Ismail, A. Recent trends of heavy metal removal from water/wastewater by membrane technologies. *J. Ind. Eng. Chem.* **2019**, *76*, 17–38. [[CrossRef](#)]
5. Liu, Y.; Ke, X.; Zhu, H.; Chen, R.; Chen, X.; Zheng, X.; Jin, Y.; Van Der Bruggen, B.; Jin, Y. Treatment of raffinate generated via copper ore hydrometallurgical processing using a bipolar membrane electrodialysis system. *Chem. Eng. J.* **2020**, *382*, 122956. [[CrossRef](#)]
6. Sun, Y.; Zhou, S.; Pan, S.-Y.; Zhu, S.; Yu, Y.; Zheng, H. Performance evaluation and optimization of flocculation process for removing heavy metal. *Chem. Eng. J.* **2020**, *385*, 123911. [[CrossRef](#)]
7. Cui, Y.; Ge, Q.; Liu, X.-Y.; Chung, N.T.-S. Novel forward osmosis process to effectively remove heavy metal ions. *J. Membr. Sci.* **2014**, *467*, 188–194. [[CrossRef](#)]
8. Duan, C.; Ma, T.; Wang, J.; Zhou, Y. Removal of heavy metals from aqueous solution using carbon-based adsorbents: A review. *J. Water Process. Eng.* **2020**, *37*, 101339. [[CrossRef](#)]
9. Qin, H.; Hu, T.; Zhai, Y.; Lu, N.; Aliyeva, J. The improved methods of heavy metals removal by biosorbents: A review. *Environ. Pollut.* **2020**, *258*, 113777. [[CrossRef](#)]
10. Shakoor, M.B.; Ali, S.; Rizwan, M.; Abbas, F.; Bibi, I.; Riaz, M.; Khalil, U.; Niazi, N.K.; Rinklebe, J. A review of biochar-based sorbents for separation of heavy metals from water. *Int. J. Phytoremediation* **2020**, *22*, 111–126. [[CrossRef](#)]
11. Baby, R.; Saifullah, B.; Rehman, F.U.; Shaikh, R.I. Greener Method for the Removal of Toxic Metal Ions from the Wastewater by Application of Agricultural Waste as an Adsorbent. *Water* **2018**, *10*, 1316. [[CrossRef](#)]
12. Cataldo, S.; Gianguzza, A.; Pettignano, A.; Piazzese, D.; Sammartano, S. Complex formation of copper(II) and cadmium(II) with pectin and polygalacturonic acid in aqueous solution. An ISE-H + and ISE-Me 2+ electrochemical study. *Int. J. Electrochem. Sci.* **2012**, *7*, 6722–6737.
13. Zhong-Kai, Y.; Chen, Y.-D.; Yang, Z.-K.; Nagarajan, D.; Chang, J.-S.; Ren, N.-Q. High-efficiency removal of lead from wastewater by biochar derived from anaerobic digestion sludge. *Bioresour. Technol.* **2017**, *246*, 142–149. [[CrossRef](#)]
14. Chouchene, A.; Jeguirim, M.; Trouvé, G. Biosorption performance, combustion behavior, and leaching characteristics of olive solid waste during the removal of copper and nickel from aqueous solutions. *Clean Technol. Environ. Policy* **2013**, *16*, 979–986. [[CrossRef](#)]

15. Mlayah, A.; Jellali, S. Study of continuous lead removal from aqueous solutions by marble wastes: Efficiencies and mechanisms. *Int. J. Environ. Sci. Technol.* **2014**, *12*, 2965–2978. [[CrossRef](#)]
16. Li, G.; Zhang, J.; Liu, J.; Sun, C.; Yan, Z. Adsorption characteristics of white pottery clay towards Pb(II), Cu(II), and Cd(II). *Arab. J. Geosci.* **2020**, *13*, 519. [[CrossRef](#)]
17. Foroutan, R.; Mohammadi, R.; Farjadfard, S.; Esmaili, H.; Saberi, M.; Sahebi, S.; Dobaradaran, S.; Ramavandi, B. Characteristics and performance of Cd, Ni, and Pb bio-adsorption using *Callinectes sapidus* biomass: Real wastewater treatment. *Environ. Sci. Pollut. Res.* **2019**, *26*, 6336–6347. [[CrossRef](#)]
18. Jellali, S.; Diamantopoulos, E.; Haddad, K.; Anane, M.; Durner, W.; Mlayah, A. Lead removal from aqueous solutions by raw sawdust and magnesium pretreated biochar: Experimental investigations and numerical modelling. *J. Environ. Manag.* **2016**, *180*, 439–449. [[CrossRef](#)]
19. Puglla, E.P.; Guaya, D.; Tituana, C.; Osorio, F.; García-Ruiz, M.J. Biochar from Agricultural By-Products for the Removal of Lead and Cadmium from Drinking Water. *Water* **2020**, *12*, 2933. [[CrossRef](#)]
20. Egirani, D.E.; Poyi, N.R.; Shehata, N. Preparation and characterization of powdered and granular activated carbon from *Palmae* biomass for cadmium removal. *Int. J. Environ. Sci. Technol.* **2020**, *17*, 2443–2454. [[CrossRef](#)]
21. Vo, A.T.; Nguyen, V.P.; Ouakouak, A.; Nieva, A.; Doma, J.B.T.; Tran, H.N.; Chao, H.-P. Efficient Removal of Cr(VI) from Water by Biochar and Activated Carbon Prepared through Hydrothermal Carbonization and Pyrolysis: Adsorption-Coupled Reduction Mechanism. *Water* **2019**, *11*, 1164. [[CrossRef](#)]
22. Ediger, V.Ş.; Berk, I.; Ersoy, M. An assessment of mining efficiency in Turkish lignite industry. *Resour. Policy* **2015**, *45*, 44–51. [[CrossRef](#)]
23. Kuśmierk, K.; Sprynskyy, M.; Świątkowski, A. Raw lignite as an effective low-cost adsorbent to remove phenol and chlorophenols from aqueous solutions. *Sep. Sci. Technol.* **2020**, *55*, 1741–1751. [[CrossRef](#)]
24. Grajales-Mesa, S.J.; Malina, G. Pilot-Scale Evaluation of a Permeable Reactive Barrier with Compost and Brown Coal to Treat Groundwater Contaminated with Trichloroethylene. *Water* **2019**, *11*, 1922. [[CrossRef](#)]
25. Zhang, W.; Gago-Ferrero, P.; Gao, Q.; Ahrens, L.; Blum, K.; Rostvall, A.; Björleinius, B.; Andersson, P.L.; Wiberg, K.; Haglund, P.; et al. Evaluation of five filter media in column experiment on the removal of selected organic micropollutants and phosphorus from household wastewater. *J. Environ. Manag.* **2019**, *246*, 920–928. [[CrossRef](#)]
26. Nazari, M.A.; Mohaddes, F.; Pramanik, B.K.; Othman, M.; Muster, T.; Bhuiyan, M.A. Application of Victorian brown coal for removal of ammonium and organics from wastewater. *Environ. Technol.* **2018**, *39*, 1041–1051. [[CrossRef](#)]
27. Zharebtsov, S.I.; Malyshenko, N.V.; Votolin, K.S.; Ismagilov, Z.R. Sorption of Metal Cations by Lignite and Humic Acids. *Coke Chem.* **2020**, *63*, 142–148. [[CrossRef](#)]
28. Binabaj, M.A.; Nowee, S.M.; Ramezani, N. Comparative study on adsorption of chromium(VI) from industrial wastewater onto nature-derived adsorbents (brown coal and zeolite). *Int. J. Environ. Sci. Technol.* **2017**, *15*, 1509–1520. [[CrossRef](#)]
29. Zhao, T.-T.; Ge, W.-Z.; Yue, F.; Wang, Y.; Pedersen, C.M.; Zeng, F.-G.; Qiao, Y. Mechanism study of Cr(III) immobilization in the process of Cr(VI) removal by Huolinhe lignite. *Fuel Process. Technol.* **2016**, *152*, 375–380. [[CrossRef](#)]
30. Pentari, D.; Perdikatsis, V.; Katsimicha, D.; Kanaki, A. Sorption properties of low calorific value Greek lignites: Removal of lead, cadmium, zinc and copper ions from aqueous solutions. *J. Hazard. Mater.* **2009**, *168*, 1017–1021. [[CrossRef](#)]
31. Uçurum, M. A study of removal of Pb heavy metal ions from aqueous solution using lignite and a new cheap adsorbent (lignite washing plant tailings). *Fuel* **2009**, *88*, 1460–1465. [[CrossRef](#)]
32. Pehlivan, E.; Arslan, G. Removal of metal ions using lignite in aqueous solution—Low cost biosorbents. *Fuel Process. Technol.* **2007**, *88*, 99–106. [[CrossRef](#)]
33. Doskočil, L.; Pekař, M. Removal of metal ions from multi-component mixture using natural lignite. *Fuel Process. Technol.* **2012**, *101*, 29–34. [[CrossRef](#)]
34. Pehlivan, E.; Richardson, A.; Zuman, P. Electrochemical Investigation of Binding of Heavy Metal Ions to Turkish Lignites. *Electroanalysis* **2004**, *16*, 1292–1298. [[CrossRef](#)]
35. Azzaz, A.A.; Jellali, S.; Assadi, A.A.; Bousselmi, L. Chemical treatment of orange tree sawdust for a cationic dye enhancement removal from aqueous solutions: Kinetic, equilibrium and thermodynamic studies. *Desalination Water Treat.* **2015**, *57*, 22107–22119. [[CrossRef](#)]
36. Azzaz, A.A.; Jeguirim, M.; Kinigopoulou, V.; Doulgeris, C.; Goddard, M.-L.; Jellali, S.; Ghimbeu, C.M. Olive mill wastewater: From a pollutant to green fuels, agricultural and water source and bio-fertilizer—Hydrothermal carbonization. *Sci. Total. Environ.* **2020**, *733*, 139314. [[CrossRef](#)] [[PubMed](#)]
37. Haddad, K.; Jeguirim, M.; Jerbi, B.; Chouchene, A.; Dutournié, P.; Thevenin, N.; Ruidavets, L.; Jellali, S.; Limousy, L. Olive Mill Wastewater: From a Pollutant to Green Fuels, Agricultural Water Source and Biofertilizer. *ACS Sustain. Chem. Eng.* **2017**, *5*, 8988–8996. [[CrossRef](#)]
38. Havelcová, M.; Mizera, J.; Sýkorová, I.; Pekař, M. Sorption of metal ions on lignite and the derived humic substances. *J. Hazard. Mater.* **2009**, *161*, 559–564. [[CrossRef](#)]
39. Huber, M.; Badenberger, S.C.; Wulff, M.; Drewes, J.E.; Helmreich, B. Evaluation of Factors Influencing Lab-Scale Studies to Determine Heavy Metal Removal by Six Sorbents for Stormwater Treatment. *Water* **2016**, *8*, 62. [[CrossRef](#)]
40. Kumar, P.S.; Korving, L.; Keesman, K.J.; Van Loosdrecht, M.C.; Witkamp, G.-J. Effect of pore size distribution and particle size of porous metal oxides on phosphate adsorption capacity and kinetics. *Chem. Eng. J.* **2019**, *358*, 160–169. [[CrossRef](#)]

41. Pn, I.; Cp, U. Overview on the Effect of Particle Size on the Performance of Wood Based Adsorbent. *J. Biosens. Bioelectron.* **2016**, *7*, 1–4. [[CrossRef](#)]
42. Jellali, S.; Wahab, M.A.; Anane, M.; Riahi, K.; Jedidi, N. Biosorption characteristics of ammonium from aqueous solutions onto *Posidonia oceanica* (L.) fibers. *Desalination* **2011**, *270*, 40–49. [[CrossRef](#)]
43. Pentari, D.; Vamvouka, D. Cadmium Removal from Aqueous Solutions Using Nano-Iron Doped Lignite. *IOP Conf. Ser. Earth Environ. Sci.* **2019**, *221*, 012135. [[CrossRef](#)]
44. Shrestha, S.; Son, G.; Lee, S.H. Kinetic Parameters and Mechanism of Zn (II) Adsorption on Lignite and Coconut Shell-Based Activated Carbon Fiber. *J. Hazard. Toxic Radioact. Waste* **2014**, *18*, 1–8. [[CrossRef](#)]
45. Pardo-Botello, R.; Fernández-González, C.; Pinilla-Gil, E.; Cuerda-Correa, E.M.; Gómez-Serrano, V. Adsorption kinetics of zinc in multicomponent ionic systems. *J. Colloid Interface Sci.* **2004**, *277*, 292–298. [[CrossRef](#)]
46. Jellali, S.; Wahab, M.A.; Ben Hassine, R.; Hamzaoui, A.H.; Bousselmi, L. Adsorption characteristics of phosphorus from aqueous solutions onto phosphate mine wastes. *Chem. Eng. J.* **2011**, *169*, 157–165. [[CrossRef](#)]
47. Haddad, K.; Jellali, S.; Jaouadi, S.; Benlifa, M.; Mlayah, A.; Hamzaoui, A.H. Raw and treated marble wastes reuse as low cost materials for phosphorus removal from aqueous solutions: Efficiencies and mechanisms. *Comptes Rendus Chim.* **2015**, *18*, 75–87. [[CrossRef](#)]
48. Haddad, K.; Jellali, S.; Jeguirim, M.; Trabelsi, A.B.H.; Limousy, L. Investigations on phosphorus recovery from aqueous solutions by biochars derived from magnesium-pretreated cypress sawdust. *J. Environ. Manag.* **2018**, *216*, 305–314. [[CrossRef](#)]
49. Gürses, A.; Hassani, A.; Kıranşan, M.; Açışlı, Ö.; Karaca, S. Removal of methylene blue from aqueous solution using by untreated lignite as potential low-cost adsorbent: Kinetic, thermodynamic and equilibrium approach. *J. Water Process. Eng.* **2014**, *2*, 10–21. [[CrossRef](#)]
50. Allen, S.J.; Brown, P.A. Isotherm analyses for single component and multi-component metal sorption onto lignite. *J. Chem. Technol. Biotechnol.* **1995**, *62*, 17–24. [[CrossRef](#)]
51. Karabulut, S.; Karabakan, A.; Denizli, A.; Yürüm, Y. Batch removal of copper(II) and zinc(II) from aqueous solutions with low-rank Turkish coals. *Sep. Purif. Technol.* **2000**, *18*, 177–184. [[CrossRef](#)]
52. Sun, H.; He, X.; Wang, Y.; Cannon, F.S.; Wen, H.; Li, X. Nitric acid-anionic surfactant modified activated carbon to enhance cadmium(II) removal from wastewater: Preparation conditions and physicochemical properties. *Water Sci. Technol.* **2018**, *78*, 1489–1498. [[CrossRef](#)] [[PubMed](#)]
53. Pekař, M.; Klučáková, M. Comparison of Copper Sorption on Lignite and on Soils of Different Types and Their Humic Acids. *Environ. Eng. Sci.* **2008**, *25*, 1123–1128. [[CrossRef](#)]
54. Singh, S.; Kumar, V.; Datta, S.; Dhanjal, D.S.; Sharma, K.; Samuel, J.; Singh, J. Current advancement and future prospect of biosorbents for bioremediation. *Sci. Total. Environ.* **2020**, *709*, 135895. [[CrossRef](#)] [[PubMed](#)]
55. Chakraborty, R.; Asthana, A.; Singh, A.K.; Jain, B.; Susan, A.B.H. Adsorption of heavy metal ions by various low-cost adsorbents: A review. *Int. J. Environ. Anal. Chem.* **2020**, 1–38. [[CrossRef](#)]
56. Leyva-Ramos, R.; Bernal-Jacome, L.; Acosta-Rodriguez, I. Adsorption of cadmium(II) from aqueous solution on natural and oxidized corncob. *Sep. Purif. Technol.* **2005**, *45*, 41–49. [[CrossRef](#)]
57. Krishnani, K.K.; Meng, X.; Christodoulatos, C.; Boddu, V.M. Biosorption mechanism of nine different heavy metals onto biomatrix from rice husk. *J. Hazard. Mater.* **2008**, *153*, 1222–1234. [[CrossRef](#)] [[PubMed](#)]
58. Demessie, B.; Sahle-Demessie, E.; Sorial, G.A. Cleaning Water Contaminated With Heavy Metal Ions Using Pyrolyzed Biochar Adsorbents. *Sep. Sci. Technol.* **2015**, *50*, 2448–2457. [[CrossRef](#)]
59. Villaescusa, I.; Fiol, N.; Martínez, M.; Miralles, N.; Poch, J.; Serarols, J. Removal of copper and nickel ions from aqueous solutions by grape stalks wastes. *Water Res.* **2004**, *38*, 992–1002. [[CrossRef](#)]
60. Zhang, C.; Li, J.; Chen, Z.; Cheng, F. Factors controlling adsorption of recalcitrant organic contaminant from bio-treated coking wastewater using lignite activated coke and coal tar-derived activated carbon. *J. Chem. Technol. Biotechnol.* **2017**, *93*, 112–120. [[CrossRef](#)]
61. Zhang, N.; Shen, Y. One-step pyrolysis of lignin and polyvinyl chloride for synthesis of porous carbon and its application for toluene sorption. *Bioresour. Technol.* **2019**, *284*, 325–332. [[CrossRef](#)]
62. Zhang, B.; Chen, Y. Particle size effect on pore structure characteristics of lignite determined via low-temperature nitrogen adsorption. *J. Nat. Gas Sci. Eng.* **2020**, *84*, 103633. [[CrossRef](#)]
63. Kanca, A. Investigation on pyrolysis and combustion characteristics of low quality lignite, cotton waste, and their blends by TGA-FTIR. *Fuel* **2020**, *263*, 116517. [[CrossRef](#)]
64. Qi, Y.; Hoadley, A.F.; Chaffee, A.L.; Garnier, G. Characterisation of lignite as an industrial adsorbent. *Fuel* **2011**, *90*, 1567–1574. [[CrossRef](#)]
65. Azzaz, A.A.; Jellali, S.; Bengharez, Z.; Bousselmi, L.; Akrou, H. Investigations on a dye desorption from modified biomass by using a low-cost eluent: Hysteresis and mechanisms exploration. *Int. J. Environ. Sci. Technol.* **2019**, *16*, 7393–7408. [[CrossRef](#)]